Review

Journal of Vibration and Control
2018, Vol. 24(9) 1587–1599

DOI: 10.1177/1077546317714882
journals.sagepub.com/home/jvc
SAGE

On nonlinear dynamics of a parametrically excited pendulum using both active control and passive rotational (MR) damper

AM Tusset[1], FC Janzen[2], V Piccirillo[1], RT Rocha[3], JM Balthazar[2,4] and G Litak[5,6]

Abstract

This paper presents two control strategies for a parametrically excited pendulum with chaotic behavior. One of them considers active control obtained by nonlinear saturation control (NSC) and the other a passive rotational magnetorheological (MR) damper. Firstly, the active control problem was formulated in order to design the external torque for the pendulum, considering the NSC. Numerical simulations were carried out in order to show the effectiveness of this method for the active control of the pendulum oscillation. The ability of the control of the proposed NSC in suppression of the chaotic behavior, considering the proposed parameters, was tested by a sensitivity analysis to parametric uncertainties. In the case of the passive rotational MR damper, firstly the influence of the introduction of the MR in a pendulum was performed considering the 0-1 test. Different electric currents are applied to suppress the chaotic behavior of the system. The numerical results showed that the simple introduction of a passive rotational MR damper without electric current did not change the chaotic behavior of the system. However, it is possible to keep the pendulum oscillating with periodic behavior using the rotational MR damper with energizing discontinuity.

Keywords

Electromechanical system, nonlinear saturation control, Dahl model, rotational magnetorheological damper, nonlinear control, chaos, 0-1 test

1. Introduction

The dynamics of a parametrically excited pendulum has been investigated for some time (Clifford and Bishop, 1995, 1996; Lu, 2006; Lenci et al., 2008, Litak et al., 2008b). Without control action the pendulum may exhibit different types of behavior, ranging from periodic to chaotic oscillations (Kecik and Warminski, 2012), as verified by Xu et al. (2005) and Litak et al. (2010).

The parametrically excited pendulum converts the outside vibration to oscillations and rotations (Bishop and Clifford, 1994). This conversion can be applied to energy harvesting (Wiercigroch, 2005). Alevras et al. (2015) investigated the capability of rotational motion appearance excited by low frequency ocean waves.

In Lenci and Rega (2011), an experimental apparatus to simulate the parametrically excited pendulum

[1]Department of Mathematics, Federal Technological University of Paraná (UTFPR), Ponta Grossa, PR, Brazil
[2]Department of Mechanical Engineering, São Paulo State University (UNESP), Bauru, SP, Brazil
[3]Department of Electronics, Federal Technological University of Paraná (UTFPR), Ponta Grossa, PR, Brazil
[4]Department of Mechanical Engineering, Technological Institute of Aeronautics (ITA), São José dos Campos, SP, Brazil
[5]Faculty of Mechanical Engineering, Lublin University of Technology, Poland
[6]Department of Process Control, AGH University of Science and Technology, Cracow, Poland

Received: 18 August 2016; accepted: 19 May 2017

Corresponding author:
AM Tusset, Department of Mathematics, Federal Technological University of Paraná, UTFPR, 84016-210 Ponta Grossa, PR, Brazil.
Email: tusset@utfpr.edu.br

was studied. The results showed a chaotic behavior and, by comparing the experimental results with the dynamical integrity profiles, it was found that experimental rotations exist only where a measure of dynamical integrity accounting for both attractor robustness and basin compactness is large enough, so that they can support experimental imperfections leading to changes in the initial conditions.

Iliuk et al. (2013) considered the introduction of a pendulum in a portal frame with nonideal excitation, with the objective of suppressing the chaotic behavior of the system, considering a pendulum as a passive controller. The results obtained by the numerical simulation showed that the chaotic behavior was suppressed and that periodic portal frame movements provide the regulated energy captured with the use of a piezoelectric material coupled to the structure.

In Stilling and Szyszkowski (2002), the control of the angular oscillations of a system considering the mass reconfiguration was examined using a pendulum of variable length. The passive control is accomplished by sliding the end mass away from the pivot as the pendulum oscillates. Simple rules relating the sliding motion to angular oscillations were proposed and evaluated through some numerical simulations.

Sieber et al. (2008) applied a standard feedback control to continuous periodic orbits. They demonstrated how initial stable rotations of a parametrically excited pendulum can be moved to an unstable region with a change of the system parameters.

However, in Yokoi and Hikihara (2011), delayed feedback control was implemented to an experimental setup of a parametric pendulum to maintain periodic rotations. Wang and Jing (2004) used the Lyapunov function method to design a controller of a pendulum system able to lead the chaotic motion to a desired periodic motion. Theoretical results were illustrated by numerical simulations which show the effect of the control.

In Tusset et al. (2016), the dynamical interactions of a double pendulum arm and an electromechanical shaker with chaotic behavior was investigated. In order to suppress the chaotic motion, the state-dependent Riccati equation (SDRE) control and nonlinear saturation control (NSC) techniques were applied.

Therefore, this paper proposes the elimination of the chaotic behavior of a parametrically excited pendulum by considering two control strategies. The first one uses active control obtained through the NSC strategy, and the second one considers a rotational magnetorheological (MR) damper modeled by the Dahl model with passive rotational MR damper. Saturation control, proposed by several researchers (Golnaraghi, 1991; Nayfeh, 2000; Oueini et al., 1997; Oueini, 1999; Pai and Schulz, 2000), was studied by Pai et al. (1998) using 2:1 internal resonance. Moreover, the use of saturation phenomena to suppress steady-state vibrations of a system by connecting it to a second-order controller using quadratic position coupling terms was studied by Felix et al. (2005).

The MR fluid (MRF) is composed of micro-sized magnetic particles, located inside a liquid carrier, that form chain-like structures when an external magnetic field is applied, resulting in an increase of the apparent viscosity of the fluid (Avraam et al., 2010). In the initial state, the fluid has a viscosity similar to low viscosity oil. Upon activation with a magnetic flux, it changes to a thick consistency (Senkal and Gurocak, 2010).

One model that has been used to describe a rotational MR damper is the Dahl model (Altenborn et al., 2014). The model consists of first-order nonlinear differential equations that approach to hysteresis loops that are experimentally observed. The Dahl model is significantly simpler and has well established conditions to ensure its physical and mathematical consistency and requires less computational time for simulations (Aguirre Carvajal et al., 2010).

The organization of this paper is as follows. Section 2 demonstrates the mathematical model of the system, and numerical simulations necessary to analyze the dynamics of the system are carried out. In Section 3, the proposed active control is designed, implemented, and the robustness of the control is analyzed considering parametric errors. Section 4 presents the application of the rotational MR damper model and the torque variation by varying the electric current applied to the control, and the rotational MR damper is considered as a passive damper. Moreover, the dynamic analysis of the passive rotational MR damper is performed through the test 0-1. The conclusions are given in Section 5.

2. Parametrically excited pendulum model

In this section, the mathematical modeling of the parametrically excited pendulum is detailed. A representation of the parametric pendulum model is illustrated in Figure 1.

The mathematical model of the parametric pendulum shown in Figure 1 has the following form (Xu et al., 2005):

$$\ddot{q} + \frac{c}{m}\dot{q} + \left(\frac{g}{l_p} + \frac{x}{l_p}\Omega^2\cos(\Omega t)\right)\sin(q) = T(t) \quad (1)$$

The angle of the pendulum is represented by q (rad), the length by l_p (m), m is the mass (kg), x (m) is the excitation amplitude, and Ω (rad s^{-1}) is the excitation frequency; c (N s m^{-1}), is the viscous damping

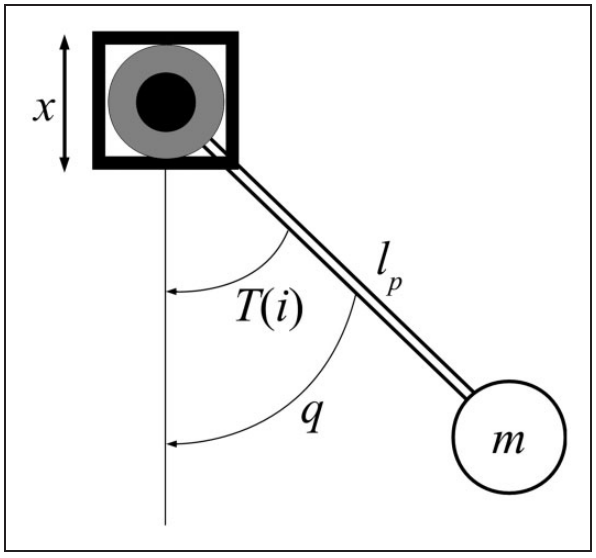

Figure 1. Schematic diagram of the parametric pendulum.

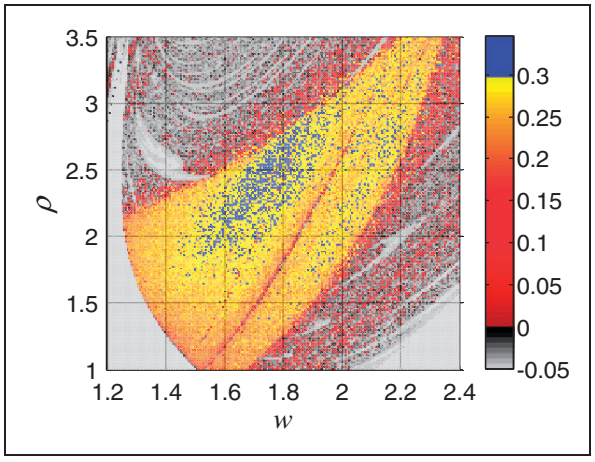

Figure 2. Largest Lyapunov exponent for various w and ρ values while $\gamma = 0.1$. The initials conditions are $x_1(0) = 0.0314$ and $x_2(0) = 0$.

coefficient, t (s) is time, g ($\mathrm{m\,s^{-2}}$) gravity acceleration, and T is the external torque (such as damping, control torque, and other loads) (Nandakumar et al., 2012).

In general, the equations are considered in terms of dimensionless variables. A dimensionless process related to the system's natural frequency ω_0 was carried out giving the dimensionless mathematical model of the parametrically excited pendulum (Nandakumar et al., 2012; Xu et al., 2005):

$$\ddot{q} + \gamma\dot{q} + (1 + \rho\cos(wt))\sin(q) = aT \tag{2}$$

where $\omega_0 = \sqrt{\frac{g}{l_p}}$, $\tau = \omega_0 t$, $\gamma = \frac{c}{m\omega_0}$, $\rho = \frac{x\Omega^2}{l_p\omega_0^2}$, $w = \frac{\Omega}{\omega_0}$, and $a = \frac{1}{\omega_0^2}$.

Equation (2) can be rewritten in state-space form as follows:

$$\begin{aligned} \dot{x}_1 &= x_2 \\ \dot{x}_2 &= -\gamma x_2 - (1 + \rho\cos(w\tau))\sin(x_1) + aT \end{aligned} \tag{3}$$

where $x_1 = q$ and $x_2 = \dot{q}$.

The next subsection will show the numerical simulations of the parametrically excited pendulum without the external torque.

2.1. Numerical simulations of the system without external torque

First, Figure 2 provides an illustration on how the parameters w and ρ in equation (3) influence the dynamics of the system, neglecting the external torque ($aT = 0$) and for the following parameter ($\gamma = 0.1$) and initials conditions $x_1(0) = 0.0314$ and $x_2(0) = 0$. The highest Lyapunov exponent estimated using the Jacobian along the trajectory (Wolf et al., 1985) shows that the dynamic system has a large region of chaotic behavior with a maximum of trajectories divergence for $w \approx 1.7$ and $\rho \approx 2.5$.

Depending on the values of w and ρ, the oscillations of the equation (3) can exhibit periodic or chaotic behaviors. Considering the parameters $\gamma = 0.1$, $\rho = 2.256281$, $w = 1.634171$, and $aT = 0$, Figure 3 shows the analysis of equation (3), considering the time history of the displacement and velocity, phase plane, Poincaré map, power spectral density, and Lyapunov exponents.

The time histories of the pendulum's displacement, x_1, and velocity, x_2, illustrated in Figure 3(a) to (c), show a nonperiodic response of the examined system. Moreover, the phase plane illustrated by Figure 3(d) represents a nonperiodic behavior.

Through the Poincaré map, the power spectral density (FFT), and the Lyapunov exponents shown in Figure 3(e) to (g), respectively, it can be deduced that the system possesses a chaotic orbit for the chosen w parameter.

As the chaotic behavior of the system was found, observing that there are many other chaotic behaviors in this region, depending on the value of w, a control strategy is designed in the next section.

3. Proposed control for parametrically excited pendulum

In this section, as the chaotic behavior of equation (3) is an undesired behavior, a control was designed by introducing a torque control signal ($aT = u$) in the pendulum system as follows:

$$\begin{aligned} \dot{x}_1 &= x_2 \\ \dot{x}_2 &= -\gamma x_2 - (1 + \rho\cos(w\tau))\sin(x_1) + u \end{aligned} \tag{4}$$

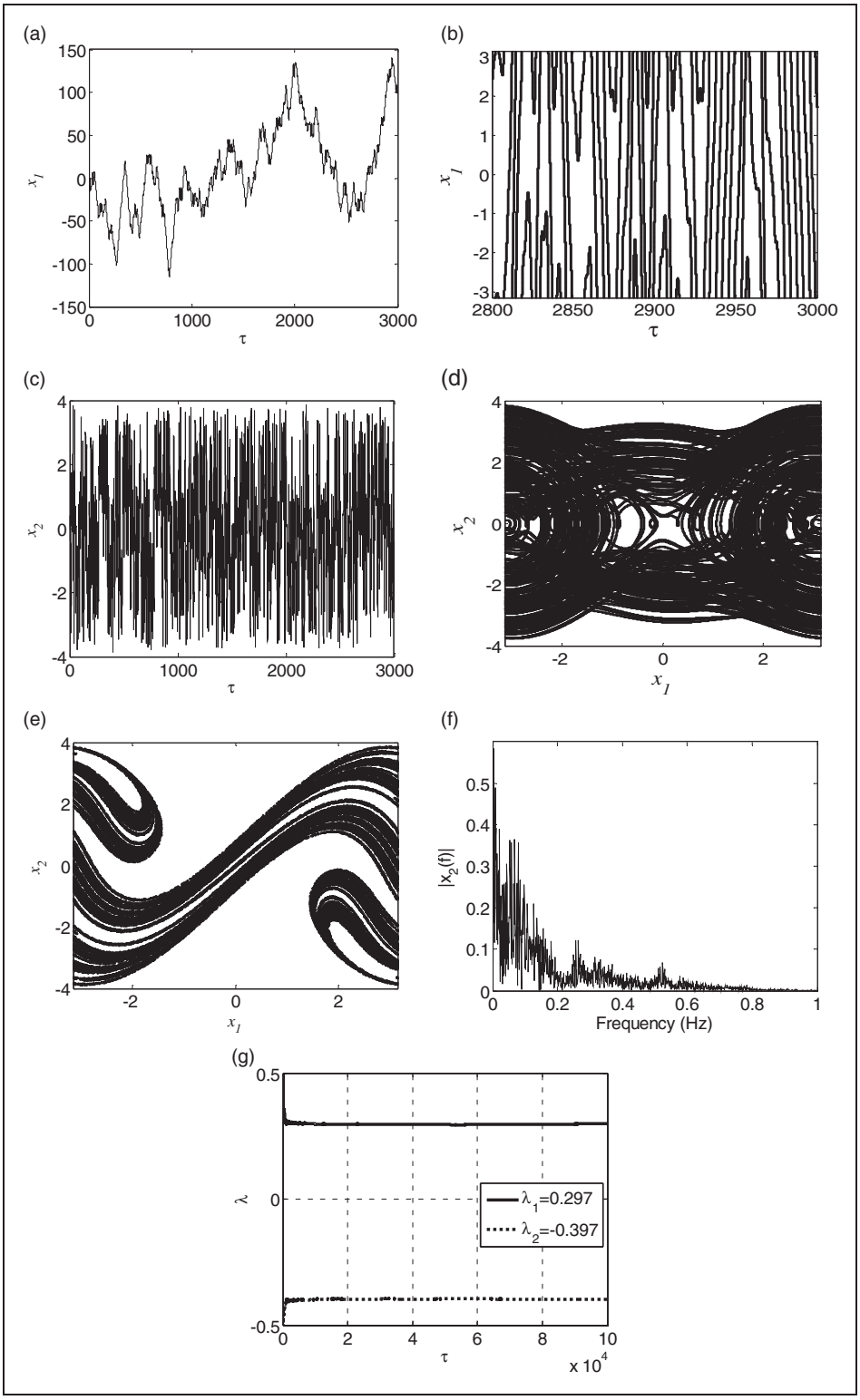

Figure 3. (a) Time history of the states x_1. (b) Time history of the states to x_1 from $[-\pi, \pi]$. (c) Time history of the states x_2. (d) Phase portrait to x_1 from $[-\pi, \pi]$. (e) Poincare map to x_1 from $[-\pi, \pi]$. (f) Power spectral density (FFT) to x_2. (g) Lyapunov exponents for regular and chaotic solutions.

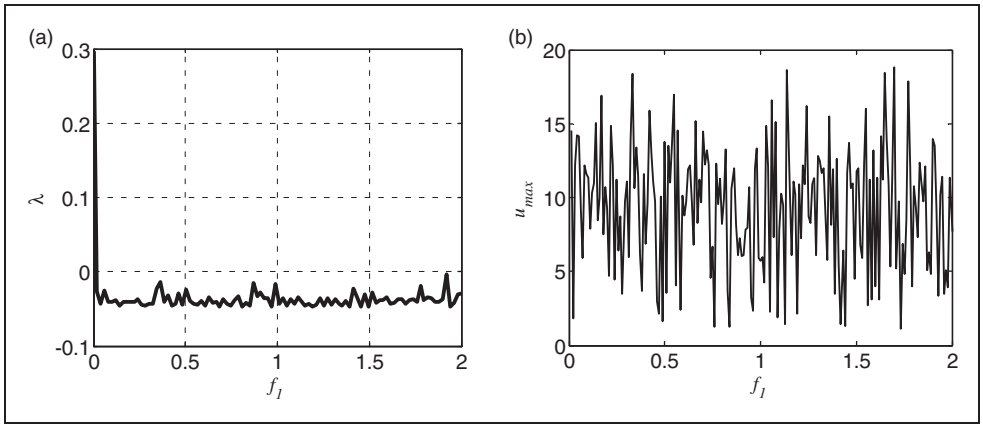

Figure 4. (a) Most significant Lyapunov exponent (calculated for $\tau = 0 : 0.01 : 10000$). (b) Control signal variation ($u_{\max}$ represents the peak value).

To control the dynamic behavior of the pendulum system, a strategy similar to that proposed by Felix et al. (2005) is considered. In this approach, the NSC (u) can be obtained from the following equation:

$$u = f_1 y^2 \tag{5}$$

where y is given by

$$\ddot{y} + \mu_c \dot{y} + \omega_c^2 y = f_2 x y \tag{6}$$

where ω_c, μ_c, f_1, and f_2 are positive constants (Felix et al., 2005). In addition, ω_c, which is considered the controller's natural frequency in equation (6), depends on the external resonance (w) of equation (4), and the internal resonance condition is considered by letting $2\omega_c \approx w$ (Felix et al., 2005, Tusset et al., 2016). As the control is proposed for equation (4), the parameters of the equation (6) will also be in dimensionless form, and the external resonance is $w = 1.634171$.

The active nonlinear vibration absorber based on the saturation phenomenon was originally developed to control vertical motions. Thus x of equation (6) is the vertical displacement for a second-order damped oscillator subjected to a harmonic excitation (Oueini *et al.*, 1997), and is used to control the vertical motions in a portal frame (x of equation (6) is the same as the vertical displacement) (Felix et al., 2005).

As the interest of this work is to apply the control of rotational motions, it will be proposed to consider $x = \sin(x_1)$, where x_1 is the angle of the pendulum, transforming angular motion into a motion similar to oscillatory displacement, making it possible to apply the control for systems with rotational movements. In this way, the proposed control of rotational motions is analogous to the control proposed by Felix et al. (2005), with the same property of internal resonance condition ($2\omega_c \approx w$) considered in Oueini et al. (1997) and Felix et al. (2005).

To use the minimum of energy to the control (u), the selection of the parameter (f_1) will depend on the lower control signal (u) which leads the chaotic behavior of the system to a periodic behavior.

Figure 4 shows the variation of the most significant Lyapunov exponent for the control system (u) as well as the control signal variation, considering $y(0) = 0.01$, $\dot{y}(0) = 0.01$, $\omega_c = \frac{w}{2} = 0.8170855$, and by detuning $u_c = 0.08$, $f_2 = 1$, and $f_1 = 0 : 0.01 : 2$.

Using $f_1 = 1.73$, the used control is minimum ($u_{\max} = 1.0964$) and it leads the system to a periodic behavior.

In Figure 5, the behavior of equation (4) can be observed with the proposed control (equation (5)) considering $f_1 = 1.73$. The application of the NSC was efficient in driving the system to a periodic behavior. The pendulum with the proposed control has a continuous rotation in a clockwise direction (Figure 5(a)), keeping the velocity always positive (Figure 5(c)).

In Figure 6, the variation of the control signal (u) can be observed. It is possible to observe that the control signal is positive (Figure 6(a)); this is a characteristic of the NSC control (see equation (5)) that has the quadratic term (y^2) and the parameter f_1 is positive constant (Felix et al., 2005); the maximum variation of the control signal is $0 \leq u \leq 1.0964$ and the regime is $0 \leq u \leq 0.7$.

3.1. Proposed control with parametric uncertainties

As the proposed control is based on parameters determined by means of detuning, the dynamic behavior of the system may not be perfectly controlled because the considered parameters may contain parametric uncertainties.

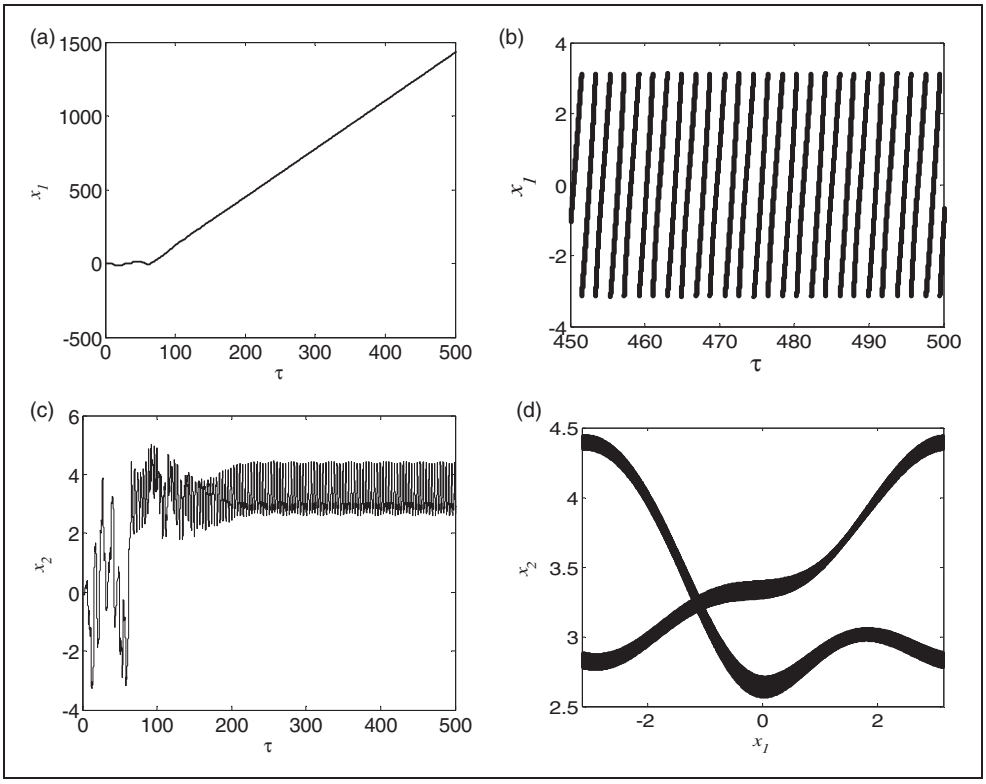

Figure 5. Movements of the pendulum with the proposed control: (a) angle of the pendulum (x_1); (b) angle of the pendulum (modulo operation $(\frac{x_1}{2\pi})$) from $x_1 \in [-\pi, \pi]$; (c) angular velocity (x_2); (d) phase diagram to (modulo operation $(\frac{x_1}{2\pi})$) from $x_1 \in [-\pi, \pi]$ versus x_2.

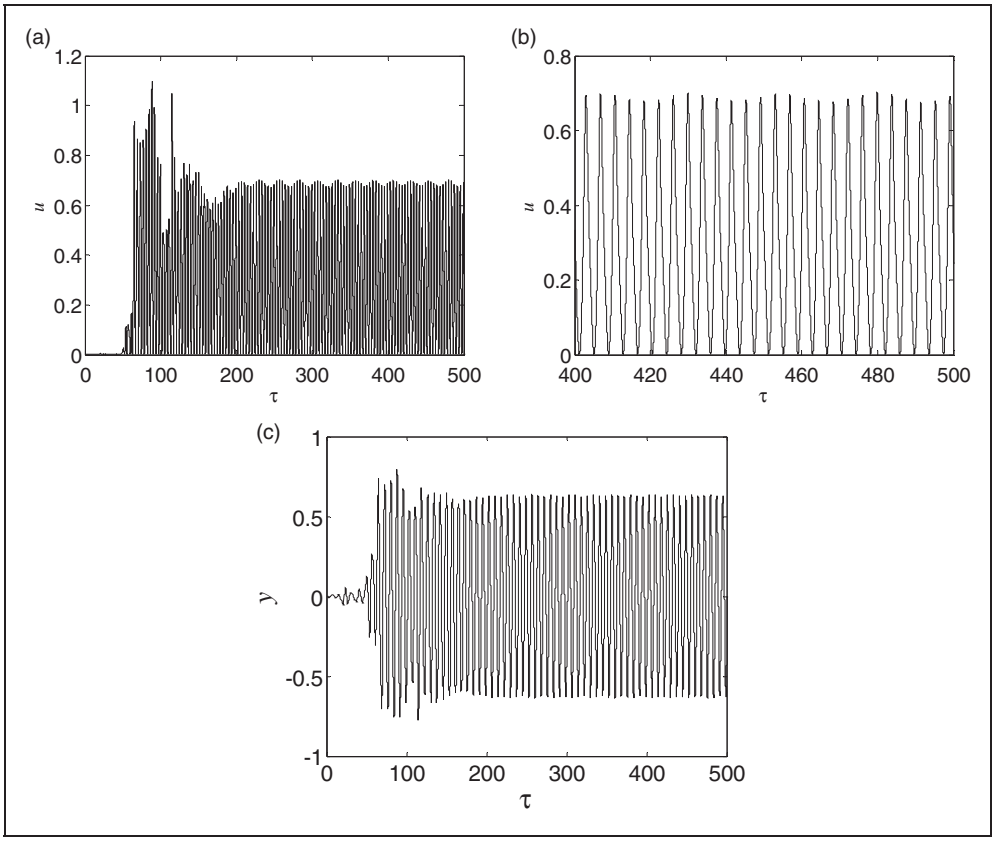

Figure 6. (a, b) Time dependence of the torque given by equation (5) with $u = 1.73\,y^2$ ($0 \leq u \leq 1.0964$). (c) Time history of the y parameter.

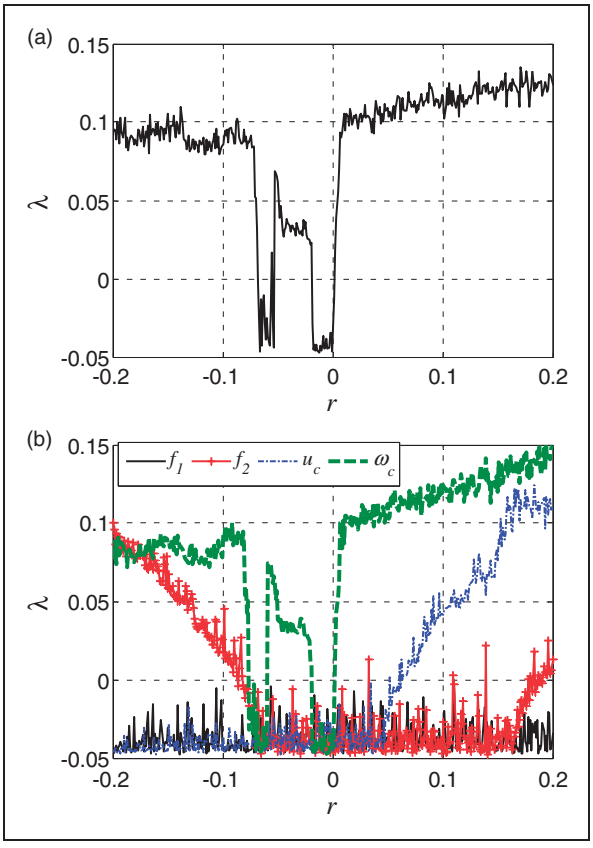

Figure 7. Most significant Lyapunov (largest) exponent. (a) Variation of parameters (u_c, f_1, f_2 and ω_c). (b) Individual variation of parameters.

In order to determine the effects of uncertainties on the performance of the controller, an error of ±20% was estimated for the parameters (u_c, f_1, f_2, and ω_c), with a strategy similar to that used by previous researchers (Balthazar et al., 2012, 2014a, 2014b; Nozaki et al., 2013; Tusset et al., 2013, 2016).

In Figure 7(a), the capacity is observed of the control to maintain the system in a periodic orbit, considering the NSC control with variation of parameters: $\mu_c = 0.08(1+r)$, $f_1 = 1.73(1+r)$, $f_2 = (1+r)$, and $\omega_c = 0.8170855(1+r)$, where $r = [-0.2, 0.2]$, considering that all the parameters are changed simultaneously according to the variation of the parameter r. Moreover, Figure 7(b) considers the uncertainty in individual variation of parameters (u_c, f_1, f_2 and ω_c), being considered that, in this case, only one of the parameters is changed according to the variation of the parameter r, while the other parameters remain constant, and without uncertainties.

The variation of the highest Lyapunov exponent (λ) is significant, demonstrating that NSC control is sensitive to variations in the parameters of the control signal (equations (5) and (6)), not being able to maintain the system in a periodic orbit. Analyzing Figure 7(a) (largest Lyapunov exponent for the simultaneous variation in the parameters) and (b) (largest Lyapunov exponent for the individual variation in the parameters), the similarity between the results of Figure 7(a) and the green result of Figure 7(b) (variation in ω_c) is observed, demonstrating that the most influential parameter is the frequency ω_c. This influence is due to the fact that to ensure the stability of the control it is necessary the internal resonance condition be $2\omega_c \approx w$, where w is the external resonance (Tusset et al., 2016).

4. Torque control using MRF

As can be seen from numerical results using a passive damper, a damper makes it possible to control the pendulum movement through the torque (Nandakumar et al., 2012). The strategy of torque control is based on MR actuators (Senkal and Gurocak, 2010). The MR actuator has several advantages, such as high yield stress, good stability, fast response time, and simple control form, it is possible to produce a high desired torque from a small brake, and it is commercially available (Senkal and Gurocak, 2010). According to Huang et al. (2002), the mechanical properties of MRFs can be used in the construction of magnetically controlled devices such as the MRF rotary brake or clutch. In the high frequency limit, the singularities in the damping dependence on velocity are terminated (Litak et al., 2008a).

Aguirre Carvajal et al. (2010) used the Dahl model to represent a MR damper applied in a portal frame with two degrees of freedom. The results showed a good match between experimental results and forces predicted by the Dahl model. Altenborn et al. (2014) considered a rotational MR damper model using the Dahl model applied in a suspension model. Numerical simulations and experimental application demonstrate that the Dahl model is appropriate for MR applications.

The Dahl model is the Coulomb friction element in the change of friction of the force when the direction of motion is changed. The Dahl model for a rotational MR damper is described as follows (Altenborn et al., 2014):

$$T_{MR} = (b_1 + b_2 i)\dot{q} + (k_1 + k_2 i)z \tag{7}$$

$$\dot{z} = \rho(\dot{q} - |\dot{q}|z) \tag{8}$$

where T_{MR} is the torque (N m), $\dot{q}$ is the angular velocity (equation (2); rad s^{-1}), z is the internal state variable (rad), i is the electric current (A), the parameters that control the shape of the hysteresis loop are b_1

(N s m^{-1}), b_2 (N s m^{-1}), k_1 (N s m^{-1}), and k_2 (N s m^{-1}), and ρ is constant.

In Figure 8, the numerical simulations results of the Dahl model (equation (7)) are shown for the following parameters: $b_1 = 0.0001$ N s m^{-1}, $b_2 = 0.05$ N s m^{-1}, $k_1 = 0.025$ N s m^{-1}, $k_2 = 0.25$ N s m^{-1}, and the constant $\rho = 5$.

Here the mechanical torque is plotted as a function of the angular velocity. It shows the hysteretic behavior with a global inclination dependent on the electric current.

4.1. Passive rotational MR damper application

Considering equation (3) with $aT = -T_{MR}$, where T_{MR} is obtained using equation (7), equation (3) is represented in the following form:

$$\begin{aligned} \dot{x}_1 &= x_2 \\ \dot{x}_2 &= -\gamma x_2 - (1 + \rho\cos(w\tau))\sin(x_1) - T_{MR} \end{aligned} \tag{9}$$

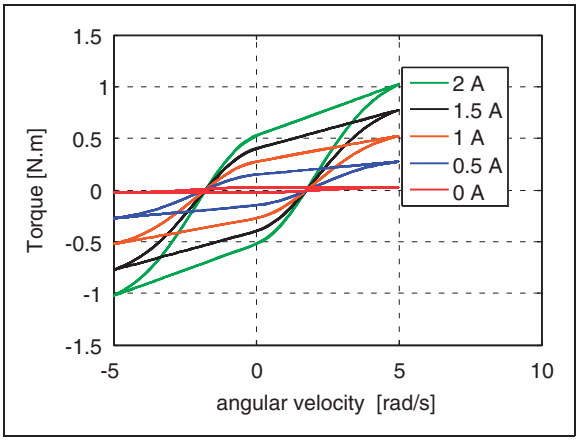

Figure 8. Characteristics of the rotational MR damper as a function of electric current.

A bifurcation diagram is built in Figure 9 by varying the electric current (i) applied in T_{MR} of equation (9) considering the range $0 \leq i \leq 2$. The behavior of the system for electric currents near zero tends to chaotic behavior. As the electric current increases, the system tends to a periodic orbit. In this range of the electric current, the application of the 0-1 test in the variable x_2 will be considered.

In Figure 9(a), as expected, with the increase of the electric current the chaotic behavior is eliminated and the system becomes periodic, behavior that was also observed by Tusset et al. (2015). However, despite higher electric currents entailing a greater hysteresis loop and hardening, which is known to reduce the amplitude of the displacement in many systems, in this case this behavior is not observed, since, as observed in Figure 9(b), with the addition of the current it is possible to obtain displacements superior to those observed with smaller currents, eliminating the chaotic behavior and without the whole elimination of the oscillatory movements.

The 0-1 test, proposed by Gottwald and Melbourne (2004, 2005), is directly applied to the time series data based on the statistical properties of a single coordinate (herein, the variable x_2 (see equation (9)).

The 0-1 test can be applied to any systems to identify chaotic dynamics (Gottwald and Melbourne, 2004, 2005; Bernardini and Litak, 2015). This test uses the temporal series data to characterize the dynamics of a system, analyzing its spectral and statistical properties based on the asymptotic properties of a Brownian motion. The 0-1 test is very useful in systems where the Lyapunov exponents are very difficult to calculate. The 0-1 test has been successfully used in the analysis of the chaotic regimes of shape memory alloy hysteretic oscillators (Litak et al., 2009, 2013; Bernardini et al., 2013).

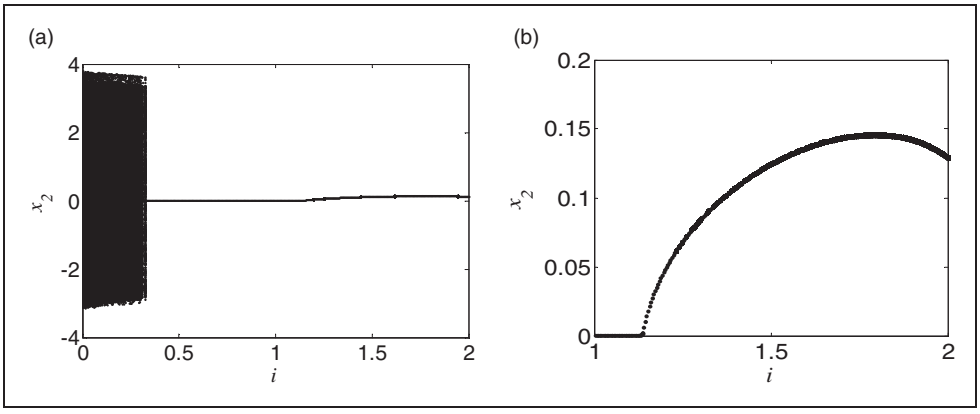

Figure 9. (a) Bifurcation diagram for $0 \leq i \leq 2$. (b) Bifurcation diagram for $1 \leq i \leq 2$.

Basically, the 0-1 test consists of estimating a single parameter K. The test considers a system variable x_j, where two new coordinates (p, q) are defined as follows:

$$p(n,\ \bar{c}) = \sum_{j=0}^{n} x(j)\cos(j\bar{c}) \tag{10}$$

$$q(n,\ \bar{c}) = \sum_{j=0}^{n} x(j)\sin(j\bar{c}) \tag{11}$$

where $\bar{c} \in (0,\ \pi)$ is a constant. The mean square displacement of the new variables $p(n,\ \bar{c})$ and $q(n,\ \bar{c})$ is given by:

$$M(n,\ c) = \lim_{n\to\infty} \frac{1}{N}\sum_{j=1}^{N}\Big[(p(j+n,\bar{c}) - p(j,\bar{c}))^2. \\ +(q(j+n,\bar{c}) - q(j,\bar{c}))^2\Big] \tag{12}$$

where $n = 1, 2, \ldots, N$ and, therefore, we obtain the parameter K_c in the limit of a very long time (Gopal et al., 2013):

$$K_c = \frac{\mathrm{cov}(Y,\ M(\bar{c}))}{\sqrt{\mathrm{var}(Y)\mathrm{var}(M(\bar{c}))}} \tag{13}$$

where $M(\bar{c}) = [M(1,\ \bar{c}),\ M(2,\ \bar{c}), \ldots, M(n_{\max},\ \bar{c})]$ and $Y = [1, 2, \ldots, n_{\max}]$.

Given any two vectors x and y, the covariance $\mathrm{cov}(x,\ y)$ and variance $\mathrm{var}(x)$ of $n_{\max}$ elements are usually defined as (Litak et al., 2013):

$$\mathrm{cov}(x, y) = \frac{1}{n_{\max}}\sum_{n=1}^{n_{\max}}(x(n) - \bar{x})(y(n) - \bar{y}) \tag{14}$$

$$\mathrm{var}(x) = \mathrm{cov}(x,\ x) \tag{15}$$

where $\bar{x}$ and $\bar{y}$ are the averages of $x(n)$ and $y(n)$, respectively. As a final result, the value of the wanted parameter K is obtained by taking the median of 100 different values of the parameter $\bar{c} \in (0, \pi)$ in equations (10) and (11). If the K value is close to 0 the system is periodic; on the other hand, if K value is close to 1 the system is chaotic. In all simulations, $n = 10{,}000$ and $j = \frac{n}{100}, \ldots, \frac{n}{10}$.

In Figure 10, the variation of K obtained by varying the current may be observed in the range $0 \le i \le 2$. The pendulum movement maintains the periodic behavior ($K \approx 0$) for any $0.33 \le i \le 2$. These results are compatible with those observed in the bifurcation diagram of Figure 9.

In Figure 11, the phase diagram can be observed, considering the cases of current $i = 0$, $i = 0.32$, and $i = 0.33$, respectively, in Figure 11(a) through (c).

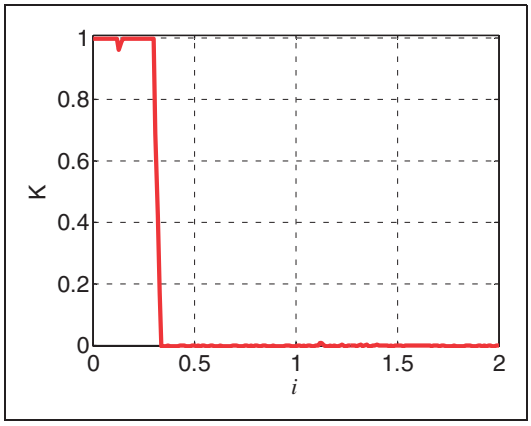

Figure 10. Variation of the K(0–1 test) parameter for $0 \le i \le 2$.

The introduction of rotational MR damper did not alter the chaotic behavior of the system (equation (3) with $aT = 0$), keeping the system with almost the same behavior for the unenergized rotational MR damper ($i = 0$, in equation (9)). Moreover, even using the current $i = 0.32$ (passive rotational MR damper), the system keeps the chaotic behavior (Figure 11(b)).

Analyzing Figure 11(c), when applying the current $i = 0.33$ the system will have a periodic behavior although with almost zero amplitude, which leads the system to a periodic behavior of the passive control that almost cancels out the movement of the pendulum, such behavior that in most cases is not indicated.

Analyzing Figure 9, it can be observed that for a higher electric current, the pendulum has an angular velocity greater than that observed for $i = 0.33$. Figure 12(a) shows the behavior of the pendulum considering $i = 1.792$, whose electric current allows the greater angular velocity, and Figure 12(b) shows the behavior of the pendulum for $i = 2$, which is the greatest electric current considered in the analysis of the behavior of the pendulum. Figure 12(c) shows the variation of $x_2 = \dot{q}$, z, and T_{MR} of equations (7) and (8), for $i = 1.792$ and Figure 12(d) shows the variation of $x_2 = \dot{q}$, z, and T_{MR} for $i = 2$.

As can be observed in Figure 12, for $i = 1.792$ it is possible to obtain a higher angular velocity and displacement than observed when using $i = 2$. If a higher torque can also be observed, being that the torque variation for $i = 1.792$ is $-0.2418 < T_{MR} < 0.2405$, and to the torque variation for $i = 2$ being $-0.2297 < T_{MR} < 0.2315$, then, such torque is required to maintain the system, equation (9), with periodic behavior (Figure 12(a) and (b)). However, it is necessary to maintain the rotational MR damper energized with current $i = 1.792$ continuously, which according to Piccirillo et al. (2015) is not intended for MR systems.

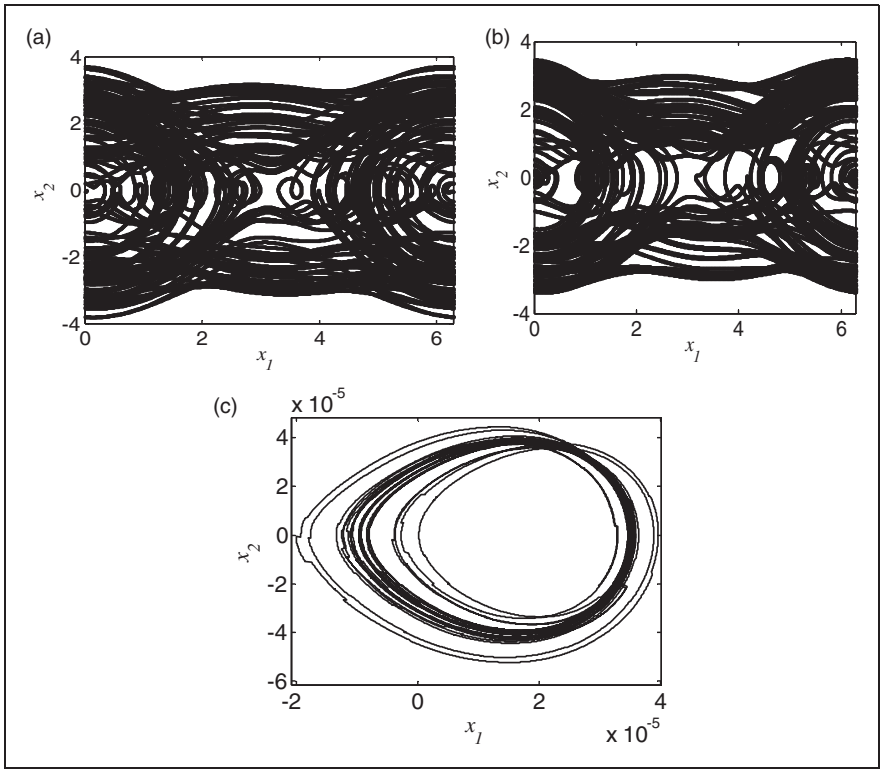

Figure 11. Phase diagrams of the pendulum with passive control: (a) phase diagram to x_1 from $[-\pi, \pi]$ with $i = 0$; (b) phase diagram to x_1 from $[-\pi, \pi]$ with $i = 0.32$; (c) phase diagram for $i = 0.33$.

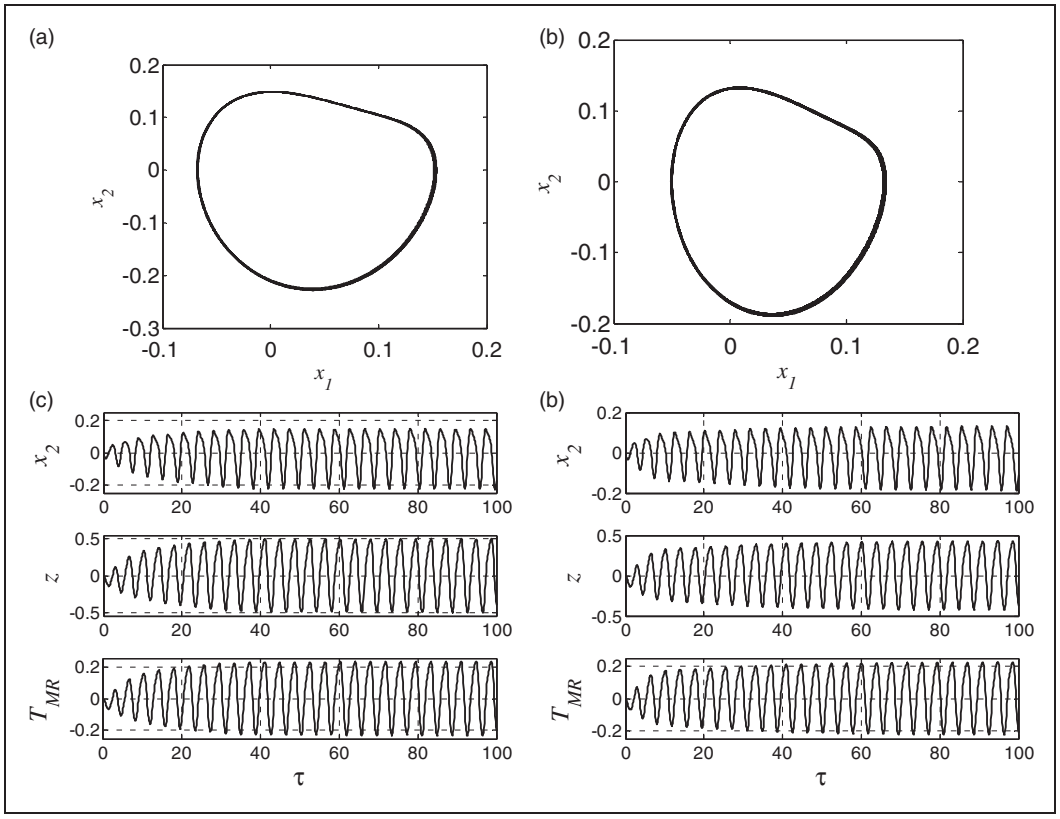

Figure 12. (a) Phase diagram for $i = 1.792$. (b) Phase diagram for $i = 2$. (c) x_2, z, and torque obtained by passive rotational MR damper for $i = 1.792$. (d) x_2, z, and torque obtained by passive rotational MR damper for $i = 2$.

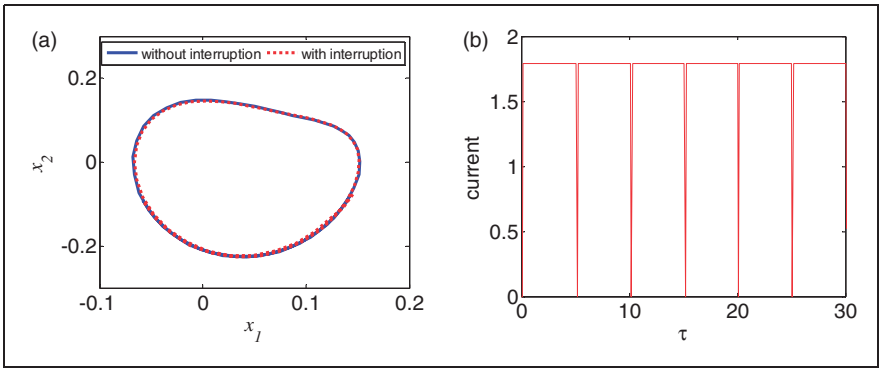

Figure 13. (a) Phase diagram for $i = 1.792$, considering with and without interruption of the current. (b) Current applied in rotational MR damper.

In Figure 13, the torque applied in equation (9) can be observed for a passive rotational MR damper (equation (7)). For the case where it energizes the rotational MR damper with $i = 1.792$, the system remains energized in a period of 5τ; after that, the energy decreases to zero in a fast moment, during 0.5τ, thus avoiding having to keep the rotational MR damper energized all the time.

As can be observed in Figure 13, the de-energization of 0.5τ (10% of the energization time) did not generate a significant difference between the results obtained with the continuous energization of $i = 1.792$, being an alternative to solve the problem of the continuous energization observed by Piccirillo et al. (2015).

5. Conclusions

The dynamics of a parametrically excited pendulum was investigated by means of time histories, phase planes, the power spectrum (FFT), and Lyapunov exponents, showing the existence of chaotic behavior for a certain values of parameters.

In applications where it is desirable to eliminate the chaotic behavior, the presented control technique, i.e. NSC, adapted to a rotational system, is demonstrated to be efficient for active control, and due to its quadratic term, the control generates a positive control, facilitating its application. The efficiency of the technique was demonstrated through numerical simulations in order to eliminate the chaotic behavior of the system. However, as observed in Figure 7(b), the NSC control does not maintain the system on periodic orbits for the variation of frequency ω_c, which is justified by the need of maintaining $2\omega_c \approx w$ (Tusset et al., 2016). For small variations of approximately 3.2% for the parameters u_c and f_2 considering $\omega_c = 0.8170855$, the NSC control maintains the system on a periodic orbit for any $f_1 = 1.73(1 + r)$, for $r = [-0.2, 0.2]$.

Related to the proposed passive rotational MR damper, it is possible to observe that the strategy is efficient in maintaining the pendulum with periodic behavior; however, it eliminates the rotational movement, keeping only the oscillatory. Through test 0-1, it was possible to determine the influence of the electric current on the behavior of the pendulum, and through the analysis of the bifurcation diagram obtained from the maximum angular velocity values, it was possible to determine that $i = 1.792$ is the electric current that maintains the system in a periodic movement with greater displacements, when compared with the other electric current cases.

As to the limitations of the passive rotational MR damper, the need of keeping the electric current continuously in the damper, the strategy of using a discontinuous signal of the current proved to be a good alternative, since it did not significantly alter the movement of the pendulum and enabled to interrupt the current every 5τ.

Acknowledgments

G Litak is grateful to the Technological Aeronautics Institute (ITA) for hosting this study.

Declaration of Conflicting Interests

The author(s) declared no potential conflicts of interest with respect to the research, authorship, and/or publication of this article.

Funding

The author(s) disclosed receipt of the following financial support for the research, authorship, and/or publication of this article: This work was supported by the CNPq (grant number 447539/2014-0) and by FAPESP.

References

Aguirre Carvajal N, Ikhouane F, Rodellar Benedé J, et al. (2010) Viscous+ Dahl model for MR damper characterization: a real time hybrid test (RTHT) validation. In: *Proceedings of the 14th European conference on earthquake engineering*, Ohrid, Republic of Macedonia, 30 August–3 September 2010, pp.1–8.

Alevras P, Brown I and Yurchenko D (2015) Experimental investigation of a rotating parametric pendulum. *Nonlinear Dynamics* 81(1–2): 201–213.

Altenborn KA, Klausen A, Tordal SS, et al. (2014) Firefly optimization used to identify hysteresis parameter on rotational MR-damper. In: *Proceedings of the international conference on mechatronics and control* (ICMC), Jinzhou, China, 3–5 July 2014, pp.2302–2307. IEEE.

Avraam M, Horodinca M, Romanescu I, et al. (2010) Computer controlled rotational MR-brake for wrist rehabilitation device. *Journal of Intelligent Material Systems and Structures* 21(15): 1543–1557.

Balthazar JM, Bassinello DG, Tusset AM, et al. (2014a) Nonlinear control in an electromechanical transducer with chaotic behaviour. *Meccanica* 49(8): 1859–1867.

Balthazar JM, Tusset AM and Bueno AM (2014b) Nonlinear TM-AFM control considering parametric errors in the control signal evaluation. *Journal of Theoretical and Applied Mechanics* 52(6): 93–106.

Balthazar JM, Tusset AM, Souza SLTD, et al. (2012) Microcantilever chaotic motion suppression in tapping mode atomic force microscope. *Proceedings of the Institution of Mechanical Engineers, Part C: Journal of Mechanical Engineering Science* 227(8): 1730–1741.

Bernardini D and Litak G (2015) An overview of 0-1 test for chaos. *Journal of the Brazilian Society of Mechanical Sciences and Engineering* 38(5): 1433–1450.

Bernardini D, Rega G, Litak G, et al. (2013) Identification of regular and chaotic isothermal trajectories of a shape memory oscillator using the 0-1 test. *Proceedings of the Institution of Mechanical Engineers, Part K: Journal of Multi-body Dynamics* 227(1): 17–22.

Bishop SR and Clifford MJ (1994) Approximating the escape zone for the parametrically excited pendulum. *Journal of Sound and Vibration* 172(4): 572–576.

Clifford MJ and Bishop SR (1995) Rotating periodic orbits of the parametrically excited pendulum. *Physics Letters A* 201(2–3): 191–196.

Clifford MJ and Bishop SR (1996) Locating oscillatory orbits of the parametrically-excited pendulum. *Journal of the Australian Mathematical Society Series B: Applied Mathematics* 37(3): 309–319.

Felix JLP, Balthazar JM and Brasil RMLRF (2005) On saturation control of a non-ideal vibrating portal frame foundation type shear-building. *Journal of Vibration and Control* 11(1): 121–136.

Gopal R, Venkatesan A and Lakshmanan M (2013) Applicability of 0-1 test for strange nonchaotic attractors. *Chaos* 23(2): 023123.

Golnaraghi MF (1991) Vibration suppression of flexible structure using internal resonance. *Mechanics Research Communications* 18(2–3): 135–143.

Gottwald G and Melbourne I (2004) A new test for chaos in deterministic systems. *Proceedings of the Royal Society of London A* 460(2042): 603–611.

Gottwald G and Melbourne I (2005) Testing for chaos in deterministic systems with noise. *Physica D: Nonlinear Phenomena* 212(1–2): 100–110.

Huang J, Zhang JQ, Yang Y, et al. (2002) Analysis and design of a cylindrical magneto-rheological fluid brake. *Journal of Materials Processing Technology* 129(1): 559–562.

Iliuk I, Balthazar JM, Tusset AM, et al. (2013) A non-ideal portal frame energy harvester controlled using a pendulum. *The European Physical Journal Special Topics* 222(7): 1575–1586.

Kecik K and Warminski J (2012) Chaos in mechanical pendulum-like system near main parametric resonance. *Procedia IUTAM* 5: 249–258.

Lenci S and Rega G (2011) Experimental versus theoretical robustness of rotating solutions in a parametrically excited pendulum: a dynamical integrity perspective. *Physica D: Nonlinear Phenomena* 240(9): 814–824.

Lenci S, Pavlovskaia E, Rega G and Wiercigroch M (2008) Rotating solutions and stability of parametric pendulum by perturbation method. *Journal of Sound and Vibration* 310(1): 243–259.

Litak G, Bernardini D, Syta A, et al. (2013) Analysis of chaotic non-isothermal solutions of thermomechanical shape memory oscillators. *The European Physical Journal Special Topics* 222(7): 1637–1647.

Litak G, Borowiec M and Kasperek R (2008a) Response of a magneto-reological fluid damper subjected to periodic forcing in a high frequency limit. *ZAMM-Journal of Applied Mathematics and Mechanics/Zeitschrift für Angewandte Mathematik und Mechanik* 88(12): 1000–1004.

Litak G, Borowiec M and Wiercigroch M (2008b) Phase locking and rotational motion of a parametric pendulum in noisy and chaotic conditions. *Dynamical Systems* 23(3): 259–265.

Litak G, Syta A and Wiercigroch M (2009) Identification of chaos in a cutting process by the 0–1 test. *Chaos, Solitons and Fractals* 40(5): 2095–2101.

Litak G, Wiercigroch M, Horton BW, et al. (2010) Transient chaotic behaviour versus periodic motion of a parametric pendulum by recurrence plots. *ZAMM-Journal of Applied Mathematics and Mechanics/Zeitschrift für Angewandte Mathematik und Mechanik* 90(1): 33–41.

Lu C (2006) Chaotic motions of a parametrically excited pendulum. *Communications in Nonlinear Science and Numerical Simulation* 11(7): 861–884.

Nandakumar K, Wiercigroch M and Chatterjee A (2012) Optimum energy extraction from rotational motion in a parametrically excited pendulum. *Mechanics Research Communications* 43: 7–14.

Nayfeh AH (2000) *Nonlinear Interactions*. New York: Wiley.

Nozaki R, Balthazar JM, Tusset AM, et al. (2013) Nonlinear control system applied to atomic force microscope including parametric errors. *Journal of Control, Automation and Electrical Systems* 24(3): 223–231.

Oueini SS (1999) *Techniques for controlling structural vibrations*. PhD Thesis, Virginia Tech, USA.

Oueini SS, Nayfeh AH and Golnaraghi MF (1997) A theoretical and experimental implementation of a control method based on saturation. *Nonlinear Dynamics* 13(2): 189–202.

Pai PF and Schulz MJ (2000) A refined nonlinear vibration absorber. *International Journal of Mechanical Sciences* 42(3): 537–560.

Pai PF, Wen B, Naser AS, et al. (1998) Structural vibration control using PZT patches and non-linear phenomena. *Journal of Sound and Vibration* 215(2): 273–296.

Piccirillo V, Balthazar JM, Tusset AM, et al. (2015) Characterizing the nonlinear behavior of a pseudoelastic oscillator via the wavelet transform. *Proceedings of the Institution of Mechanical Engineers, Part C: Journal of Mechanical Engineering Science* 230(1): 120–132.

Senkal D and Gurocak H (2010) Serpentine flux path for high torque MRF brakes in haptics applications. *Mechatronics* 20(3): 377–383.

Sieber J, Gonzales-Buelga A, Neild SA, et al. (2008) Experimental continuation of periodic orbits through a fold. *Physical Review Letters* 100(24): 244101.

Stilling DSD and Szyszkowski W (2002) Controlling angular oscillations through mass reconfiguration: a variable length pendulum case. *International Journal of Non-Linear Mechanics* 37(1): 89–99.

Tusset AM, Bueno AM, Nascimento CB, et al. (2013) Nonlinear state estimation and control for chaos suppression in MEMS resonator. *Shock and Vibration* 20(4): 749–761.

Tusset AM, Piccirillo V, Balthazar JM, et al. (2015) On suppression of chaotic motions of a portal frame structure under non-ideal loading using a magneto-rheological damper. *Journal of Theoretical and Applied Mechanics* 53(3): 653–664.

Tusset AM, Piccirillo V, Bueno AM, et al. (2016) Chaos control and sensitivity analysis of a double pendulum arm excited by an RLC circuit based nonlinear shaker. *Journal of Vibration and Control* 22(17): 3621–3637.

Wang R and Jing Z (2004) Chaos control of chaotic pendulum system. *Chaos, Solitons and Fractals* 21(1): 201–207.

Wiercigroch M (2005) A new concept of energy extraction from waves via parametric pendulor. Patent application, UK.

Wolf A, Swift J, Swinney H, et al. (1985) Determining Lyapunov exponents from a time series. *Physica D: Nonlinear Phenomena* 16(3): 285–317.

Xu X, Wiercigroch M and Cartmell MP (2005) Rotating orbits of a parametrically-excited pendulum. *Chaos, Solitons and Fractals* 23(5): 1537–1548.

Yokoi Y and Hikihara T (2011) Tolerance of start-up control of rotation in parametric pendulum by delayed feedback. *Physics Letters A* 375(17): 1779–1783.